

A New Biocontrol Agent *Bacillus velezensis* SF334 Against Rubber Tree Fungal Leaf Anthracnose and Its Genome Analysis of Versatile Plant Probiotic Traits

Muyuan Wang^{1,†}, Yikun Zhang^{1,†}, Haibin Cai², Xinyang Zhao³, Zhongfeng Zhu¹, Yichao Yan¹, Ke Yin¹, Guanyun Cheng¹, Yinsheng Li¹, Gongyou Chen^{1,4}, Lifang Zou^{1,4,*}, Min Tu^{2,5,*}

Table S1. The plant growth promotion-associated genes in *B. velezensis* SF334

Gene ID	KO	Gene	Function	Class
SF334GL002344	K01695	<i>trpA</i>	tryptophan synthase alpha chain	Phenylalanine, tyrosine and tryptophan biosynthesis
SF334GL003147	K14155	<i>patB, malY</i>	cysteine-S-conjugate beta-lyase	Biosynthesis of secondary metabolites
SF334GL002056	K00128	<i>aldh</i>	aldehyde dehydrogenase (NAD+)	Tryptophan metabolism
SF334GL002972	K00128	<i>aldh</i>	aldehyde dehydrogenase (NAD+)	Tryptophan metabolism
SF334GL004032	K00128	<i>aldh</i>	aldehyde dehydrogenase (NAD+)	Tryptophan metabolism
SF334GL002345	K01696	<i>trpB</i>	tryptophan synthase beta chain	Phenylalanine, tyrosine and tryptophan biosynthesis
SF334GL002347	K01609	<i>trpC</i>	indole-3-glycerol phosphate synthase	Phenylalanine, tyrosine and tryptophan biosynthesis

Table S2. General features of genomes of *B. velezensis* SF334, *B. velezensis* FZB42, *B. velezensis* SQR9, *B. amyloliquefaciens* DSM7, and *B. subtilis* 168

General features	<i>B. velezensis</i> SF334	<i>B. velezensis</i> FZB42	<i>B. velezensis</i> SQR9	<i>B. amyloliquefaciens</i> DSM7	<i>B. subtilis</i> 168
Genome size (bp)	4,078,641	3,918,596	4,117,023	3,980,199	4,227,167
GC content	46.5%	46.48%	46.10%	46.08%	43.49%
Coding density (%)	89.33	89.026	89.68	88.54	88.33
Protein coding sequences (CDS)	4,142	3,888	4,111	4,220	4,388
tRNA	86	89	72	94	86
5s rRNA	9	10	7	10	10
16s rRNA	9	9	7	10	10
23s rRNA	9	10	7	10	10
Repeat region	30	31	20	43	38

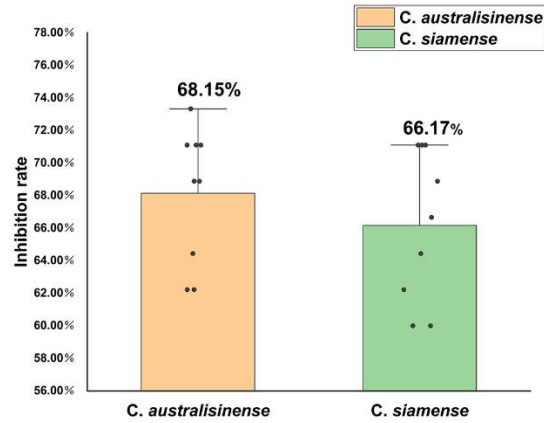


Figure S1. Antagonistic effect of strain SF334 against *C. siamense* and *C. australisense*, which are major pathogens causing leaf anthracnose of rubber trees in the Hainan province of China. The average inhibition rates of SF334 against *C. siamense* and *C. australisense* were calculated.

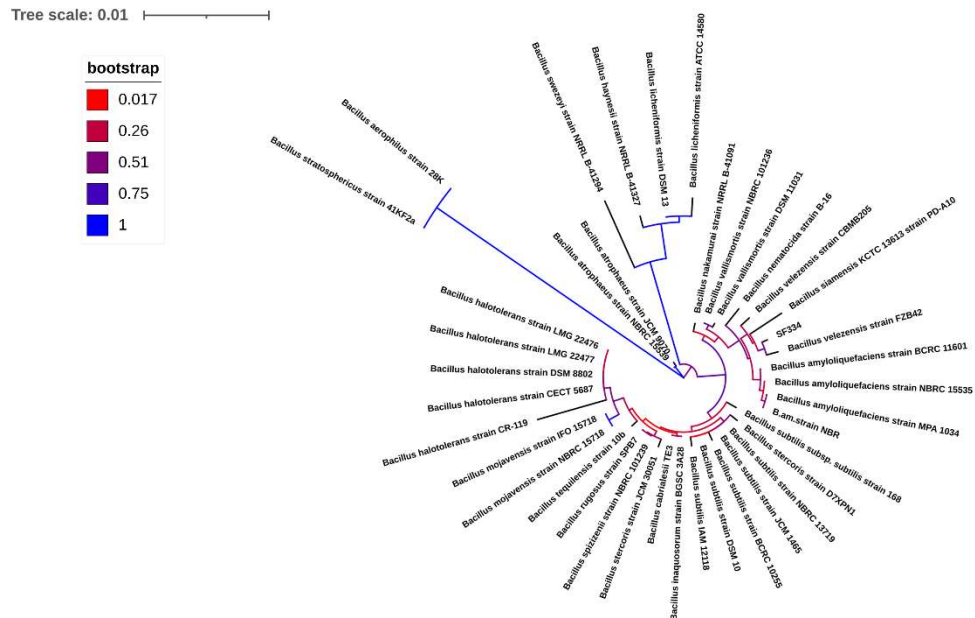


Figure S2. The phylogenetic tree of strain SF334 based on 16S rDNA sequences constructed through the TYGS platform. The sequence of 16S rRNA of 39 strains with the lowest E-value in the National Center for Biotechnology Information (NCBI) database were selected as the reference sequences. The results were finally imported into MEGA 11 soft to construct a phylogenetic tree by the NJ (1200 bootstrap) method.

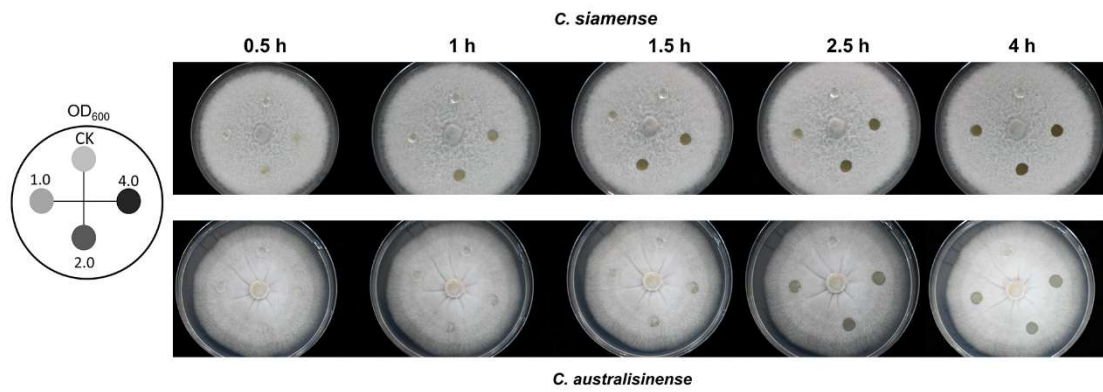


Figure S3. Observation of the hyphal lysis of *C. siamense* and *C. australisinese* when interacting with the CSs of *B. velezensis* SF334 on PDA plates. The mycelium of *C. siamense* and *C. australisinese* were inoculated with the indicated bacterial concentration for 0.5 h, 1h, 1.5 h, 2.5 h and 4 h.

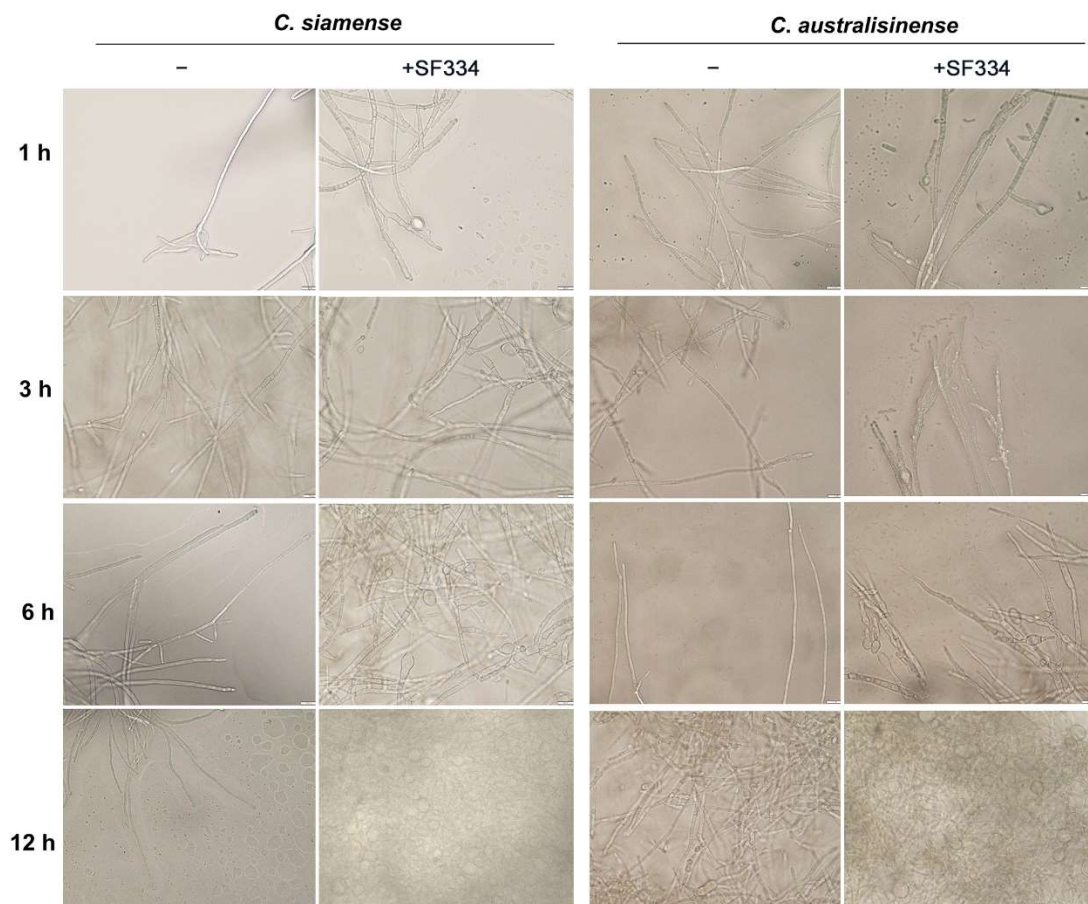


Figure S4. Observation of mycelium morphology of *C. siamense* and *C. australisinese* when interacting with the CSs of *B. velezensis* SF334 for 1 h, 3 h, 6 h, and 12 h in PDB medium using an optical microscope. Scale bar, 10 μ m.

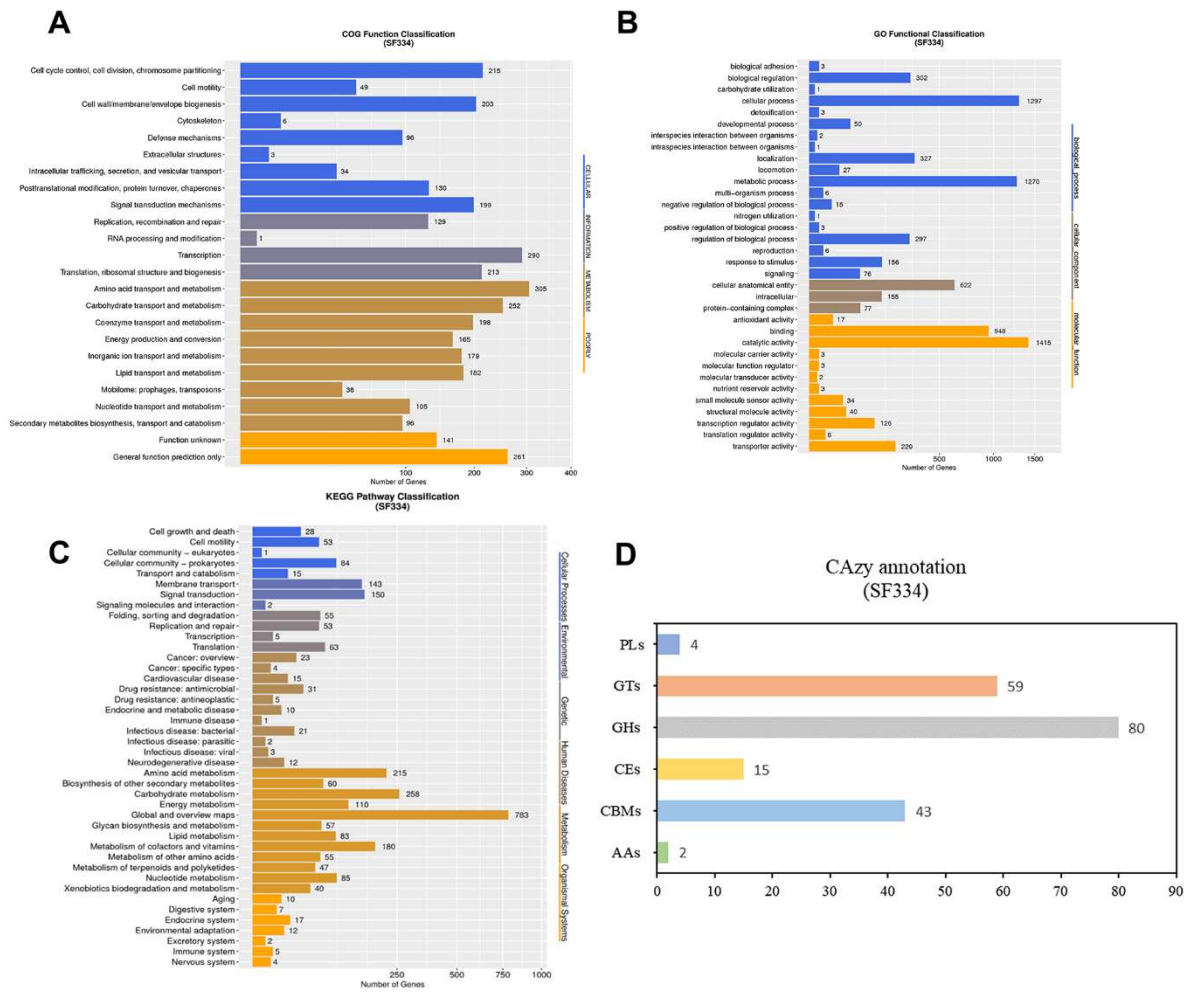


Figure S5. Genomic analysis of *B. velezensis* SF334. The COG analysis (A), GO analysis (B), KEGG pathway analysis (C) and CAZy annotation (D) of *B. velezensis* SF334

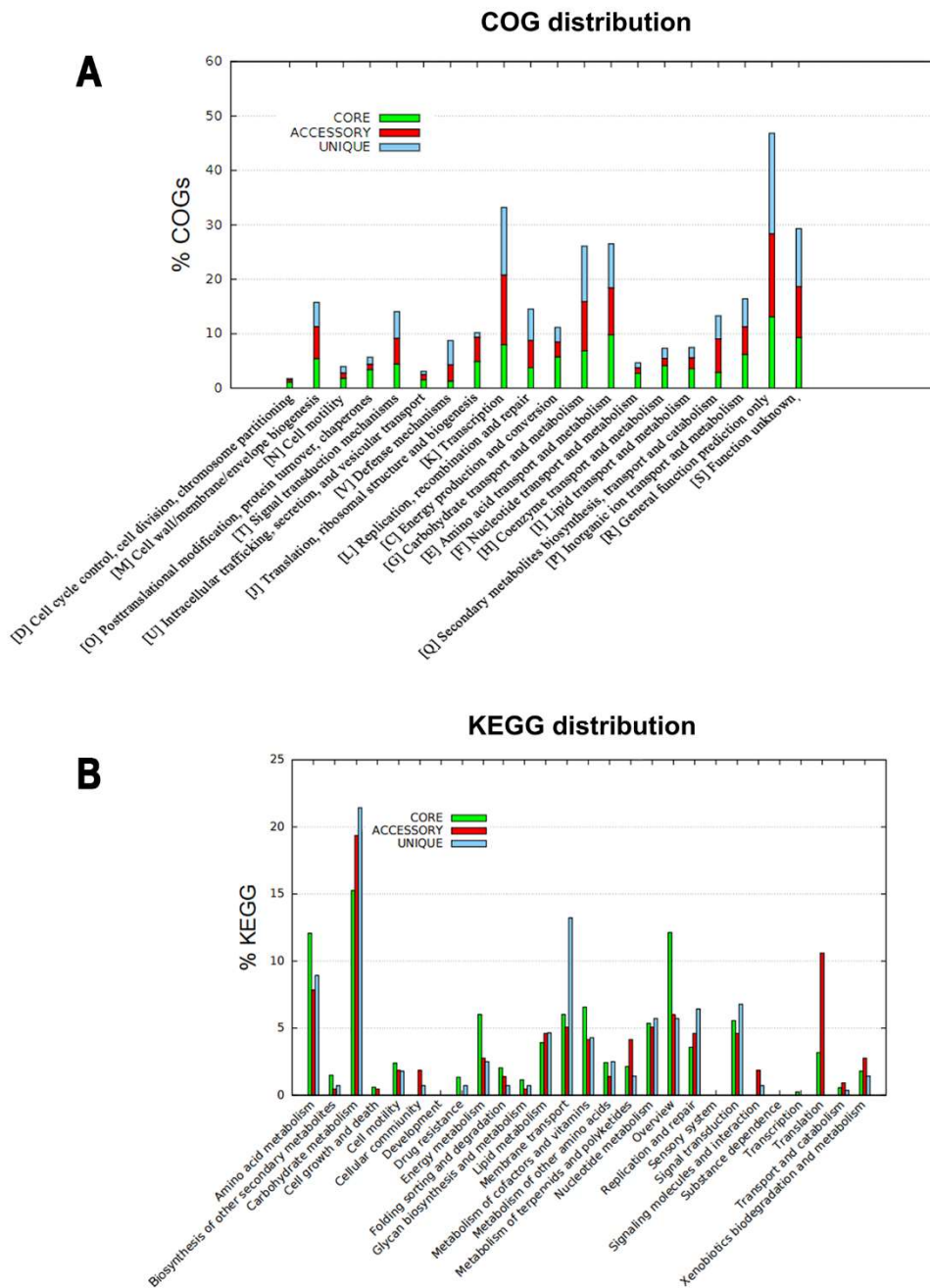


Figure S6. Comparative genomic analysis of *B. velezensis* SF334 with four other related *Bacillus* species. The COG analysis (A) and KEGG pathway analysis (B) of *B. velezensis* SF334 with *B. velezensis* FZB42, *B. velezensis* SQR9, *B. amyloliquefaciens* DSM7, and *B. subtilis* 168. Green, red and blue boxes indicate core genes, accessory and unique genes between five strains.